Can an alcohol act as an acid/base catalyst in water solution? An experimental and theoretical study of imidazole catalysis of the aqueous Morita–Baylis–Hillman reaction

Lluís Raich,[a,b,] Hugo Santos,[a,c] Juliana C. Gomes,[c] Manoel T. Rodrigues, Jr.,[c] Renan Galaverna,[d] Marcos N. Eberlin,[d] Fernando Coelho,[c,*] Carme Rovira,[a,b,e] and Albert Moyano,[a,*]*

[a] Secció de Química Orgànica, Departament de Química Inorgànica i Orgànica, Facultat de Química, Universitat de Barcelona, Martí i Franquès 1-11, 08028-Barcelona, Catalonia, Spain

[b] Institut de Química Teòrica i Computacional (IQTCUB), Facultat de Química, Universitat de Barcelona, Martí i Franquès 1-11, 08028 Barcelona, Catalonia, Spain.

[c] Laboratory of Synthesis of Natural Products and Drugs, Institute of Chemistry, University of Campinas, UNICAMP P.O. Box 6154 – 13083-970, Campinas, SP, Brazil

[d] ThoMSon Mass Spectrometry Laboratory, Institute of Chemistry, University of Campinas, UNICAMP P.O. Box 6154 – 13083-970, Campinas, SP, Brazil

[e] Institució Catalana de Recerca i Estudis Avançats (ICREA), Passeig Lluís Companys, 23, 08018 Barcelona, Catalonia, Spain.

KEYWORDS Morita-Baylis-Hillman reaction, catalysis, density functional theory, proton transfer

ABSTRACT: The formation of carbon-carbon sigma bonds by the organocatalyzed Morita-Baylis-Hillman (MBH) constitutes a sustainable way for the synthesis of valuable, highly functionalized molecules. Its large-scale implementation is however hampered both by its poor performance with substrates such as α,β-unsaturated ketones and by the reduction of the nucleophilicity of the catalyst when using water as solvent. Recent work from our laboratories has shown that a bicyclic imidazolyl alcohol (BIA), overcomes these limitations and is a much more efficient catalyst than imidazole for the aqueous MBH reactions of cyclic enones. The role of the hydroxyl group in the former catalyst is not easy to understand, however, since these reactions take place in water solution. We have studied the mechanism of the aqueous Morita-Baylis-Hillman (MBH) reaction between 2-cyclohexenone and isatin, catalyzed either by imidazole or by the BIA catalyst, using a combined experimental and computational approach. The data allowed us to propose mechanistic free-energy profiles for the two catalysts. An intramolecular proton transfer step, facilitated by the hydroxyl group of the catalyst even if the reaction takes place in water, accounts for the higher catalytic efficiency of BIA in comparison to imidazole, which requires assistance by an external base (either hydroxide ion or another imidazole molecule) for this catalytic step. The computed activation energies are in good agreement with the experimentally observed trends in reaction rates. The crucial role of the BIA hydroxyl has been confirmed by NMR study of the reaction kinetics, and *in sit*u ESI-MS/MS monitoring experiments have detected and characterized all the relevant reaction intermediates, validating the computational model. To the best of our knowledge, this is the first study that provides clear evidence for the intramolecular participation of a bifunctional catalyst in the proton transfer step of a MBH reaction. The fact that the introduction of a suitable functional group favors the intramolecular proton transfer over solvent-mediated pathways, just in the spirit of enzymatic catalysis, provides a basis for the rational design of future efficient catalysts for aqueous reactions.

1. INTRODUCTION

More than four decades after its initial discovery,[1] the Morita-Baylis-Hillman (MBH) reaction (Scheme 1) continues to draw a lot of attention, both from the practical and from the theoretical points of view.[2,3]

The MBH reaction has been established as a major method for the formation of carbon–carbon single bonds, affording highly functionalized products. The reaction also benefits from: (i) ready availability of the starting materials, and the possibility of being employed in the industrial-scale production of valuable drugs or intermediates;[4] (ii) a

superior atom-economic nature; (iii) the use of purely organic catalysts; (iv) mild reaction conditions; (v) synthetic versatility of the reaction products;[5] and (vi) potential for the development of efficient enantioselective versions.[3d,6]

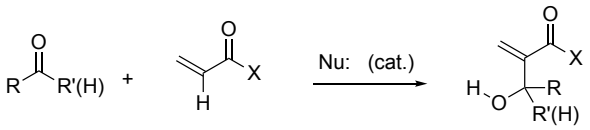

Scheme 1. The prototypical Morita-Baylis-Hillman (MBH) reaction.

Despite many advantages, MBH reactions still suffer from a few crucial practical drawbacks: (i) use of hazardous solvents and/or substrates (*Cf.* acrylate esters or acrylonitrile as solvents and reactants in the prototypical MBH reaction), (ii) high amounts (typically up to 100% mol) of the nucleophilic catalyst, and (iii) low reactivity of β-substituted activated olefins (as donors) and of ketones (as acceptors). These limitations have precluded its more general use in large-scale conditions.

Some MBH reactions involving cyclic α,β-unsaturated ketones have been particularly difficult to achieve, taking place only under harsh conditions.[7] The use of water as the solvent can alleviate some of these shortcomings, but water usually diminishes the nucleophilicity of the catalyst, so that an excess of the nucleophilic promoter is generally required in aqueous medium.[8] The reduced solubility of the organic substrates in water can also slow down the reaction rate.

The MBH reaction mechanism has been shown to involve four steps (Scheme 2).[3d,6b,9] The first step involves the conjugate addition of the nucleophile catalyst, generating a zwitterionic enolate. The second step occurs via an aldol-type addition of the carbonyl compound forming a zwitterionic alkoxide. The third step involves a carbon-to-oxygen proton transfer that generates a second zwitterionic enolate. Finally, in the fourth step, elimination of the catalyst yields the MBH adduct. Although the general features of this mechanism are well established, the specific details of each individual step –particularly those of the critical carbon-to-oxygen proton transfer, step **III** in Scheme 2– and the identification of the rate-determining step (RDS) are still under debate.[9-12] In addition, no straightforward way to improve the efficiency of actual catalysts has been devised.

Several years ago, Aggarwal[11] and McQuade[12] revised the early mechanistic proposals for the MBH reaction.[9a] On the basis both of kinetics and of isotope effects, they proposed that step **III** (proton transfer; Scheme 2) and not step **II** (carbon–carbon bond formation by aldol-type addition of the carbonyl compound), should be the RDS, contrary to the initial proposal of Hill and Issacs.[9a] The two studies suggested different mechanisms for the proton transfer step: intermolecular transfer via a "proton shuttle" mediated by a hydroxyl group (present either in the solvent or in the MBH adduct),[11] or an intramolecular proton transfer (taking place concurrently with catalyst elimination) in an intermediate hemiacetal alkoxide,[12] respectively. The intermolecular proton transfer route should be favored in protic polar solvents, whereas the intramolecular route would be more likely in MBH reactions of aldehydes taking place in aprotic media. Further experimental studies have been performed to detect proposed reaction intermediates,[9d,13] and the mechanism of the MBH reaction has also been studied computationally. Several studies have estimated either potential- or free energy-profiles along the reaction coordinate in model systems, using density functional theory and including implicit solvation effects.[9c,9d,14] These computational studies have been so far inconclusive since they either support the "proton shuttle" proposal of Aggarwal *et al.*[11] or suggest the coexistence of the two competing pathways.[9c]

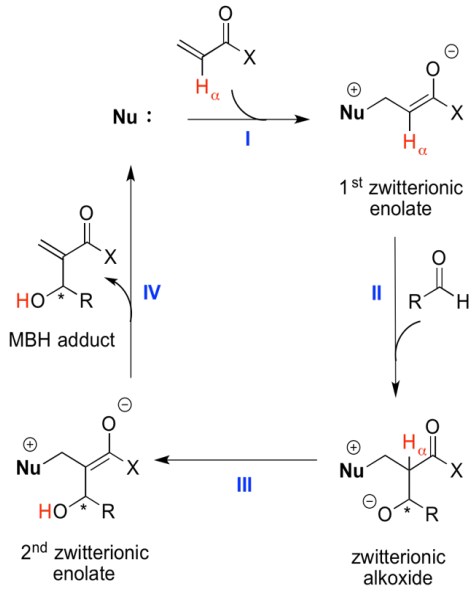

Scheme 2. Standard catalytic cycle for the MBH reaction between an aldehyde RCHO and an α,β-unsaturated carbonyl derivative CH_2=CHCOX. Step I: conjugate addition of the nucleophile catalyst. Step II: aldol-type addition of the carbonyl compound. Step III: proton transfer. Step IV: catalyst elimination

Recently, Plata and Singleton[15] reported a detailed experimental mechanistic free energy profile for the prototypical MBH reaction between *p*-nitrobenzaldehyde and methyl acrylate, using 1,4-diazabicyclo[2.2.2]octane (DABCO) as a catalyst, in methanol solution. They found that steps **II** and **III** are competitive RDS's (*i.e.*, the RDS is temperature and substrate dependent) and that a stepwise, solvent mediated acid-base mechanism (but not the concerted "proton shuttle" pathway) takes place in this case. It was also pointed out that the modeling of reaction steps involving solvent participation requires the inclusion of explicit solvent molecules to obtain meaningful results.[15,16] But it is unclear whether these considerations would apply for other catalysts and, more importantly, whether Michael acceptors such as cyclic α,β-unsaturated ketones, would display a similar mechanistic behavior.

We have shown that the use of a readily available[17] bicyclic imidazolyl alcohol (BIA) catalyst, 7-hydroxy-6,7-dihydro-5*H*-pyrrolo[1,2-*a*]imidazole (**1**), overcomes most limitations of the MBH reaction with cyclic enones, affording very good results in the aqueous MBH reaction of conjugated cycloalkenones both with aromatic and aliphatic aldehydes[18] and with isatin derivatives,[19] in the presence of sodium dodecyl sulfate as an additive.

The bicyclic imidazolyl alcohol **1** is a much more efficient catalyst than imidazole (**2**), that had been previously used in stoichiometric amounts to promote the MBH reactions of cyclic enones in the presence of water.[8] These contrasting behaviors are surprising when considering that both catalysts share a similar structure, and that they differ basically, leaving aside the extra cycle, by the presence of a hydroxyl group in **1**. Can a single hydroxyl group explain the greater catalytic efficiency of the bicyclic imidazolyl alcohol **1** with respect to imidazole **2**? The question becomes more crucial when we realize that the reaction takes place in an aqueous medium, where the proton transfer step could apparently be easily promoted by a water molecule, ruling therefore out the possibility that the hydroxyl group in the BIA catalyst **1** could play any significant role in the reaction mechanism. It is worth noting however that although proton transfer reactions between heteroatoms are extremely fast (diffusion controlled), the abstraction of the proton attached to the α carbonylic carbon by an alkoxide oxygen will in general take place with a substantial energy barrier, so that the activation energy for the proton transfer step **III** should depend on the structure of the intermediate alkoxide species involved.

In order to ascertain the role played by the hydroxyl group of the imidazolyl alcohol **1** in the catalysis of the MBH reaction of cyclic conjugated enones in water solution, we have performed a combined experimental and computational mechanistic study of the aqueous MBH reaction between isatin (**3**) and 2-cyclohexenone (**4**) using both BIA (**1**) and imidazole (**2**) as catalysts (Scheme 3). This has allowed us to propose mechanistic free-energy profiles for each catalyst that explain the observed differences in catalytic efficiency. Our results have also been checked against the intermediates "fished out" from both reactions via *in situ* monitoring performed by electrospray ionization mass spectrometry (ESI(+)-MS).

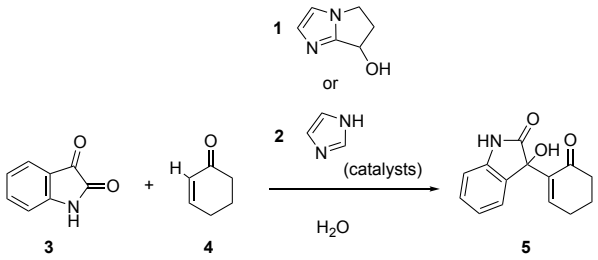

Scheme 3. MBH reactions studied in this work.

2. METHODS

2.1. NMR monitoring of the aqueous MBH reaction between isatin and 2-cyclohexenone catalyzed by imidazole-based heterocycles

To a 10 mL round-bottomed flask, equipped with a magnetic stirrer, were added sequentially isatin **3** (425 mg, 2.89 mmol), sodium dodecyl sulfate (SDS, 83 mg, 0.29 mmol), catalyst **1** or **2** (0.29 mmol), distilled H_2O (2.9 mL) and 2-cyclohexen-1-one **2** (0.56 mL, 555 mg, 5.78 mmol). The heterogeneous reaction mixture was stirred at room temperature and the reaction conversion was monitored by ^{1}H NMR spectroscopy. The progress of the reactions was also easily visualized as the reaction medium turned from an orange-colored suspension to a pale yellow one (see Supporting Information). In order to prepare the samples for NMR analysis, about 70 μL of the reaction mixture were taken, diluted with 2 mL of brine and extracted with EtOAc (2 x 5 mL). The organic phase was separated, dried over anhydrous Na_2SO_4, concentrated under reduced pressure and analyzed. The reaction conversion was estimated by measuring the ratio of the areas of the signals corresponding to the *N*-*H* proton both in isatin **3** and in the MBH adduct **5**

2.2. Quantum chemical calculations

The Gaussian09 package[20] was used for all calculations. The electronic structure was computed within density functional theory (DFT),[21] using M06-2X functional[22] and an extended 6-311++G** basis set to expand Kohn-Sham orbitals.[23] This functional is well known to provide accurate kinetics and thermodynamics for addition reactions to α,β-unsaturated ketones,[24] but to ensure its suitability for this particular system, we have tested many functionals and methods for the global MBH reaction (thermodynamics) and its first catalytic step (kinetics). Taking CCSD(T)/6-311++G** as a reference method of accuracy, the best compromise between kinetics and thermodynamics is M06-2X, with errors below 3 kcal·mol^{-1} (see SI).

A SMD solvation model,[25] parametrized for M06 functionals, was used in all calculations (energy evaluations, optimizations and frequencies), considering water as solvent. An explicit water molecule, presumably involved in the proton transfer step, was included in the calculations from the beginning to avoid accounting for non-realistic translational entropy. Sodium dodecyl sulfate has not been explicitly considered in the calculations because we have demonstrated that its role is essentially that of enhancing the solubility of the organic substrates in water, and that in the case of isatin **3** the reaction takes place essentially with the same rate in the absence of the surfactant.[19] Structure optimizations and transition state (TS) searches were performed with the Berny algorithm. Minima and TS structures were characterized by exhibiting zero and one imaginary frequency, respectively. The connections between the minimum-energy structures and the TS's were checked by analyzing the corresponding imaginary frequency modes. We have assumed a fast interconversion between the different conformers of the reaction intermediates, so that we present the lowest-energy ones

rather than the conformers directly connected to the transition states.

The reference state for all calculations (ΔG = 0 kcal·mol^{-1}) is constituted by the hydrogen-bonded complex of 2-cyclohexenone with a water molecule (**4**·H_2O), isatin (**3**) and the respective catalyst (imidazole **2** or BIA **1**), in aqueous solution and at infinite distance. For the chiral BIA catalyst **1**, we have performed our calculations with the (*R*)-configured enantiomer; when several diastereomers for a given TS or intermediate are possible, we will present in general the results corresponding to the lowest free energy pathway.

2.3. General procedure for *in situ* reaction monitoring by ESI(+)-MS

All reactions monitored by ESI(+)-MS were run in a magnetically stirred 10 mL round-bottomed flask containing 2.0 mmol of isatin (**3**), 4.0 mmol of 2-cyclohexenone (**4**), 0.20 mmol of catalyst (imidazole **2** or BIA **1**) and an aqueous solution of SDS (0.20 mmol in 2 mL of deionized water), at ambient temperature. Aliquots from the reaction medium (1 µL) were continuously taken and diluted in 1 mL of a CH_3CN-H_2O (1:1) solution. The sample solutions were prepared in polypropylene microtubes (Eppendorf®) and directly injected into the ESI(+)-MS.

2.4. ESI(+)-MS data

High-resolution MS data were obtained by means of an Agilent ifunnel Q-TOF 6550 LC–MS with source Dual Agilent Jet Stream ESI (Dual AJS-ESI) in the following conditions: drying gas temperature at 280 ºC; drying gas flow 12 L· min^{-1}; nebulizer at 30 psi; sheath gas temperature at 300 °C; sheath gas flow 12 L min^{-1}; VCap 2500 V; nozzle voltage 0 V; fragmentor 150 V; OCT 1 RF Vpp 750 V and collision energies for the MS/MS experiments were varied in a range of 15-30 V using N_2. The diluted samples were injected via a LC in FIA mode at a flow rate of 100mL·min^{-1}. Data were recorded in full MS mode using ESI(+) and a *m/z* 50 to 1000 range. Mass spectra were processed via the Mass Hunter B.06.00 software (Agilent technologies, Santa Clara, California).

3. RESULTS AND DISCUSSION

3.1. Comparative kinetic analysis of the catalysis of the MBH reaction by compounds 1 and 2.

In our previous work, we found that the BIA catalyst **1** was more efficient than imidazole **2** in the aqueous MBH reaction between isatin **3** and 2-cyclohexenone **4**, since the reaction was essentially complete after 4 h at rt when a 10% molar amount of **1** was used as a catalyst, while in the presence of a 65% molar amount of **2** the reaction had not finished after 18 h.[19] In order to have a more quantitative estimation of the relative efficiency of both catalysts, we ran two parallel reactions with a 10% mol amount of compounds **1** and **2**, respectively, and we measured the isatin/product ratio by direct ^{1}H-NMR analysis of the reaction mixture. As it can be clearly seen in Figure 1, the initial rate of the BIA-catalyzed reaction is 14.3 times higher than that of the imidazole-catalyzed one, that after 48 h at rt showed a conversion lower than 70%.

Next, and in order to see if this difference in reaction rate was due to the presence of a hydroxyl group in the BIA catalyst, we evaluated the catalytic activity of the known[17b] O-methyl derivative **6** (Figure 1).

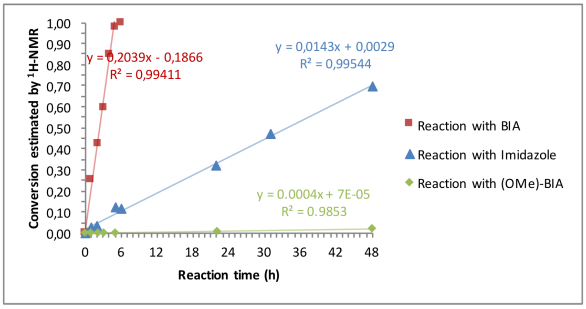

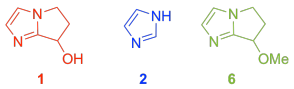

1 2 6

Figure 1. Conversion *vs.* time in the aqueous MBH reaction between isatin (**3**) and 2-cyclohexenone (**4**) with the catalysts (10 mol% amount) BIA (**1**; red squares), imidazole (**2**; blue triangles) and (OMe)-BIA (**6**; green diamonds).

We were pleased to find that the O-methylated derivative **6** had indeed a very low catalytic activity, resulting in a rate constant 500 times smaller than that observed with the hydroxyl-containing catalyst **1**. In the light of this result, however, the relatively small difference in the catalytic efficiencies between **1** and **2** was not easily rationalized, suggesting the possibility that imidazole might act not only as a nucleophilic catalyst. In another experiment, we used *N*-methylimidazole (**7**) as the catalyst in the same reaction conditions (10 mol% of **7**, 10 mol% of SDS, 2 molar equiv of 2-cyclohexenone **4** with respect to isatin **3**, water –1 mL/mmol of **3**), and we found that the reaction rate was identical to that of the imidazole-catalyzed reaction (see SI). This appears to rule out any significant participation of the imidazole NH in the mechanism.

Since the only significant difference between **6** and **2** (or **7**) lies in the degree of steric hindrance around the more basic nitrogen in both compounds, we reasoned that imidazole could also act as an external Brønsted base in the rate-determining C-H_α abstraction in step III (see Scheme 2). With the aim of verifying this hypothesis, we ran the reaction with a double amount of catalyst **2** (20 mol% *vs.* 10 mol%), and ^{1}H-NMR monitoring of the conversion showed that the reaction rate increased by a factor of almost three; the apparent order of the reaction with respect to imidazole is 1.7, clearly suggesting the existence of a competitive pathway second-order in imidazole **2**. On the other hand, when we halved the amount of BIA catalyst **1** (5 mol% *vs.* 10 mol%), the reaction rate was approximately divided by two, establishing a first-order dependence on this catalyst (see SI for details).

Taking these results into account, imidazole **1** was taken as the model nucleophilic catalyst for comparison with **2** both in the computational and in the *in situ* ESI(+)-MS studies.

3.2. Computational analysis

We will here discuss the computational results obtained for each individual step (see Scheme 2) of the aqueous MBH reaction between isatin (**3**) and 2-cyclohexenone (**4**), paying special attention to the differences between the two catalysts (BIA **1** and imidazole **2**). We have used density functional theory to depict the reaction mechanism of both catalysts. The results of our calculations are summarized in Figure 2.

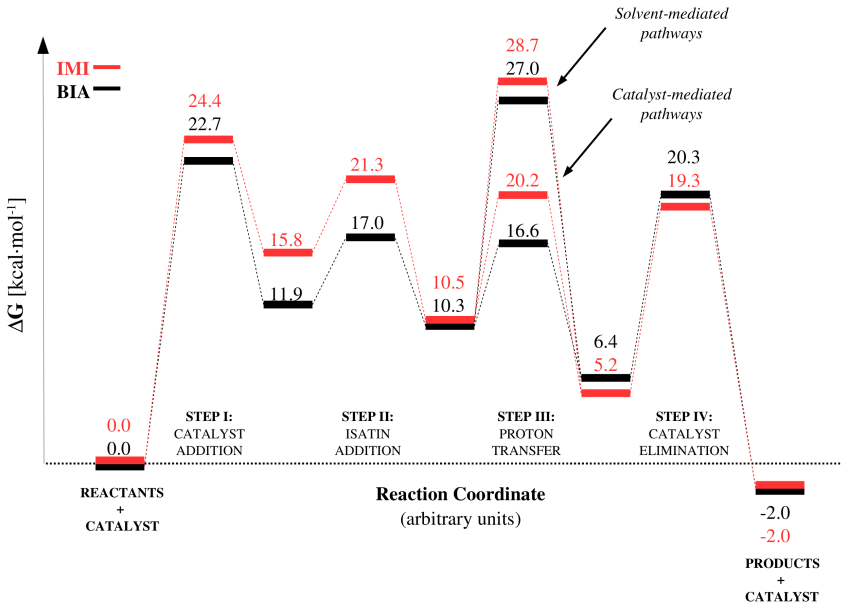

Figure 2. Calculated minimum energy reaction paths for the aqueous MBH reaction between isatin **3** and 2-cyclohexenone **4**, catalyzed by the BIA **1** (black) and by imidazole **2** (red). See Scheme 2 for the description of the individual steps

As it can be seen, the computed free energy barriers for each individual step are in general lower for the BIA catalyst **1** than for imidazole **2**. The mechanistic differences between both catalysts are especially important in the proton transfer step, so that in the following discussion we will focus our attention in this specific step. A more detailed discussion of the other steps can be found in the Supporting Information.

3.2.1. Step I: Catalyst addition.

Our study began by modeling the first step of the MBH reaction (addition of the catalyst, step I in Scheme 2), considering both BIA (**1**) and imidazole (**2**) as catalysts. Figure 3 shows the optimized structures and the free energies (relative to the reference state) of the stationary structures along the reaction pathway. The activation energy for the addition of the BIA catalyst is lower than that of imidazole ($\Delta\Delta G^{\ddagger}$ = 1.7 kcal·mol^{-1}), a fact that is in principle surprising given that both **1** and **2** should have a similar nucleophilic character, and in any case the BIA catalyst should be more sterically hindered. This unexpected lowering of the reaction barrier can be attributed to the stabilization provided by a well-defined hydrogen bond network between the hydroxyl group of the BIA catalyst, the enolate oxygen and a bridging water molecule (Figure 3). In fact, knocking out this H-bond network by reorienting the OH during the addition of BIA (**1**) to 2-cyclohexenone (**4**) leads almost to the same barrier obtained for imidazole (see SI). Although both catalysts have a similar Lewis basicity, and therefore should exhibit a similar catalytic efficiency,[26] the presence of an intermolecular hydrogen bond at the TS I-**1** seems therefore to favor the reaction for BIA over imidazole.

The bridging water molecule also has a stabilizing role in the zwitterionic intermediates Int I-**1** and Int I-**2** (Figure 3). Here, the stability difference between both catalysts is even larger ($\Delta\Delta G^{o}$ = 3.9 kcal·mol^{-1}) than that at the TS, since the negative charge at the enolate oxygen is fully developed. Interestingly, the water molecule is found to form a shorter hydrogen bond with the enolate oxygen at Int I-**1** (1.6 Å) than with the carbonyl oxygen of 2-cyclohexenone **4** (1.8 Å). As we will see later, ESI(+)-MS/MS data provide experimental evidence for the formation of these hydrated intermediates.

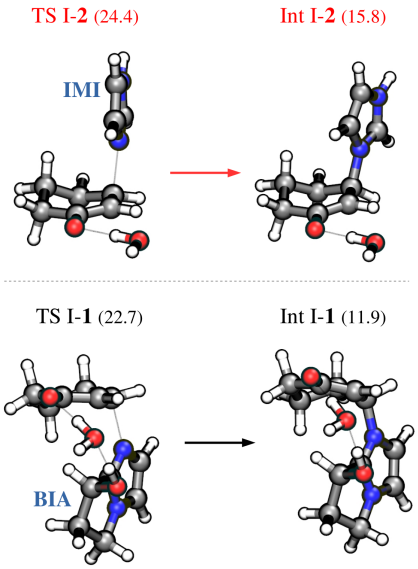

Figure 3. Free energies (kcal·mol^{-1}, relative to the reference state) and optimized structures of the stationary points (transition states and intermediate products) for the addition (step I in Scheme 2) of imidazole (IMI **2**; top) and BIA (**1**; bottom) to ciclohexenone (**3**).

The differences in the rate of this step between both catalysts are therefore related with their different ability to stabilize the nascent negative charge in the enolate oxygen of the first zwitterionic intermediate formed in step I.

3.2.2. Step II: Aldol addition of isatin.

Figure 4 shows the optimized structures and energies of the stationary states along the second step of the MBH reaction (aldol addition) for BIA and imidazole catalysts. In both cases, the reaction energy barrier is lower, and therefore not kinetically relevant, in comparison to the previous step. Nevertheless, step II is fundamental for a possible asymmetric induction by the chiral BIA catalyst, as the configuration of the chiral center of the MBH adduct **5** is defined in this step. The stereochemistry of step II is particularly complex. For a given first zwitterionic intermediate, there are in principle four possible nucleophilic attacks depending on the faces of the enolate carbon in Int I-**2** and of the isatin carbonyl that are reacting. We have explored all of these possibilities for both catalysts, and we depict in Figure 4 exclusively the lowest energy pathways. A more detailed discussion of this step can be found in the SI.

For the imidazole-catalyzed reaction, we have found that the preferred attack of isatin takes place on the less hindered face of the enolate carbon. In the minimum energy pathway, this attack involves the *Re* face of the isatin carbonyl to the *Si* face in (*R*)-Int I-**2**, leading, through the transition state TS II-**2**, to the intermediate Int II-**2** (Figure 4 top), with a computed energy barrier of $\Delta G^{\ddagger}$ = 5.5 kcal·mol^{-1}. For the (*R*)-BIA catalyst **1**, the lowest energy transition state TS II-**1** for this step involves the addition of the *Re*-face of the enolate carbon to the *Re*-face of the isatin carbonyl in **3** (Figure 4 bottom). The energy barrier corresponding to this step is of $\Delta G^{\ddagger}$ = 5.1 kcal·mol^{-1}, slightly lower than that obtained for imidazole (See Figure 2).

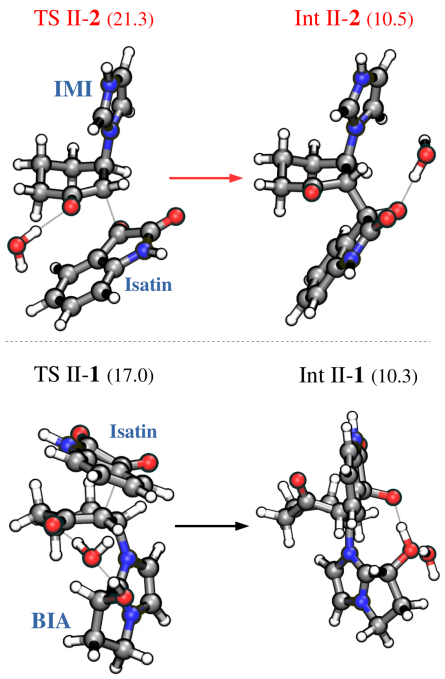

Figure 4. Free energies (in kcal·mol^{-1}) and optimized structures of the stationary points for the isatin addition (step II in Scheme 2) under catalysis by imidazole **2** (top) and by the BIA **1** (bottom).

3.2.3. Step III: Carbon to oxygen proton transfer.

The proton transfer from the α-carbon to the alkoxide oxygen (step III in Scheme 2) in intermediates Int II-**1** and Int II-**2** can occur through several pathways. A direct concerted proton transfer is unlikely in view of the high energy associated with a strained four-membered cyclic transition state.[9c] Other possible pathways are the autocatalytic product-induced proton transfer uncovered by Aggarwal,[11] or the mediation of a second electrophile molecule of McQuade.[12] These pathways are expected to be predominant in aprotic media, whereas in a protic solvent such as water, the most likely mechanism would be in principle the solvent-mediated proton transfer (path A in Scheme 4).

Furthermore, in the case of imidazole catalysis, the results of the kinetic experiments described in Section 3.1 above show that we must consider an alternative reaction pathway in which, following the fast, reversible protonation of the alkoxide oxygen in Int II-**2**, a second molecule of imidazole **2**, acting as a Brønsted base, brings about the abstraction of the C–H_{α} proton. The subsequent fast neutralization of the resulting imidazolium cation by the hydroxide anion would afford the same zwitterionic enolate intermediate (Int III-**2**) arising from the solvent-mediated proton transfer A (Path B in Scheme 4).

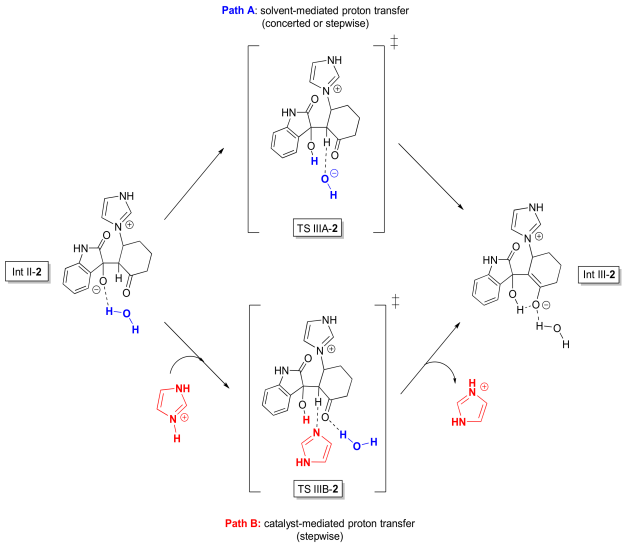

Scheme 4. Alternative proton-transfer pathways for step III in the imidazole-catalyzed reaction.

For the imidazole-catalyzed reaction starting from intermediate Int II-**2**, we have located and characterized the transition state, TS IIIA-**2**, for the water-mediated carbon to oxygen proton transfer, leading directly to the second zwitterionic enolate Int III-**2**. The transition state TS IIIA-**2** (see Figure 5 for the optimized structure) has a very high free energy (ΔG^o = 28.7 kcal·mol^{-1} with respect to the separated reactants), so that according to this mechanism step III should be rate-determining even in aqueous solution. The individual activation energy (from the aldol intermediate Int II-2) is of $\Delta G^{\ddagger}$ = 18.2 kcal·mol^{-1}, roughly 6 kcal·mol^{-1} lower than that for the catalyst addition to the enone **4**. The transfer of the α-carbon proton turns out to be very asynchronous. In the TS IIIA-**2**, the water molecule has already transferred a proton to the C3-alkoxide oxygen of the oxindole moiety, whereas the proton transfer from the α-carbonylic carbon to the hydroxide anion oxygen is still taking place. This observation led us to think that, starting from intermediate Int II-**2**, we could find a stable species in which the water molecule had completely transferred one proton to the oxindole alkoxide before reaching transition state TS IIIA-**2**. In fact, a careful examination of the reaction coordinate allowed us to find the postulated intermediate Int II'-**2**, that is 4.1 kcal·mol^{-1} less stable than Int II-**2** (see SI). However, this structure is situated in a very shallow region of the potential energy hypersurface; hence, it must be very short lived because of its essentially barrier-less (*ca.* 0.6 kcal·mol^{-1} activation energy value) reversal to Int II-**2**. From the mechanistic point of view, this previous oxygen to oxygen proton transfer is therefore irrelevant in water, and we can consider that after the conformational change the carbon to oxygen proton transfer according to path A in Scheme 4 is fully concerted.

Next, we set out to explore the reaction coordinate for the carbon to oxygen proton transfer according to path B in Scheme 4, which implies the fast and reversible protonation of the alkoxide group in Int II-**2**, followed by the abstraction of the α-carbonyl CH proton by an imidazole molecule that acts as a Brønsted base. We have located and characterized the corresponding transition state for this process, TS IIIB-**2**, and we were pleased to find that its free energy (ΔG^o = 20.2 kcal·mol^{-1}, relative in this case to that of the separated reactants plus protonated imidazole) is much lower than that of TS IIIA-**2** (See Figure 5). This is in accordance with our experimental finding that the order of the reaction is of 1.7 with respect to imidazole, due to the contribution of the proton-transfer step (of second order with respect imidazole) to the overall reaction rate.

For the reaction catalyzed by BIA **1**, we were also able to locate a transition state for the water-mediated carbon to oxygen proton transfer (TS IIIA-**1**, see Figure 5) which is similar to TS IIIA-**2**, and that also has a very high free energy (ΔG^o = 27.0 kcal·mol^{-1} relative to that of the separated reagents). A previous conformational change of Int II-**1** places the alkoxide-bound water near the proton α to the carbonyl, facilitating the proton transfer. The individual (i.e. from the starting intermediate Int II-**1**) activation free energy for this step of 16.7 kcal·mol^{-1} turned to be somewhat smaller than that ($\Delta G^{\ddagger}$ = 18.2 kcal·mol^{-1}) calculated for imidazole along pathway A in Scheme 4. In this case, the fact that the reaction rate is of first order on the BIA catalyst **1** excludes the possibility of a pathway similar to that of B in Scheme 4, involving two molecules of **1** in the transition state. We have, however, found an alternative pathway in which the BIA hydroxyl is first deprotonated by the oxindole alkoxide, and subsequently abstracts the proton α to the cyclohexanone carbonyl. The initial proton transfer from the BIA hydroxyl to the oxindole alkoxide in Int II-**1** takes place with a very low energy barrier, leading to an intermediate of nearly the same energy, that is, having a ΔG^o = 10.4 kcal·mol^{-1} with respect to the separated reactants. After a conformational change, the key carbon to oxygen proton transfer can take now place, via the transition state TS IIIB-**1** (with a free energy ΔG^o = 16.6 kcal·mol^{-1} with regard of the separated reactants, Figure 5), to the second zwitterionic intermediate Int III-**1**. The overall transformation is clearly exoergic, with ΔG^o = -3.9 kcal·mol^{-1} from Int II-**1** to Int III-**1**, and takes place with a low individual activation free energy of $\Delta G^{\ddagger}$ = 6.3 kcal·mol^{-1}.

At this point, one may ask why is TS III-B **1** more than 10 kcal·mol^{-1} more stable than TS III-A **1**? It is worth noting that this fact cannot be rationalized from the equilibrium aqueous pKa values of the hydroxyl groups implied in the proton-transfer step. In both TS's, the oxygen atoms that abstract the α-carbonylic proton (hydroxide anion for TS III-A **1** and the catalyst alkoxide for TS III-B **1**) have a net negative charge, and their relative stability will be largely dependent on solvation and polarization effects. A close inspection of the structures of TS III-A **1** and TS III-B**1** in Figure 5 reveals that they have a very similar solvent-accessible surface area around the negatively charged oxygen that abstracts the CH proton, so that solvation effects should be nearly equal for both species and that polarization effects might account for the energy difference between them.[27] In fact, when we calculated the natural charges in both transition states, we were pleased to find that while the α-carbonylic carbon and the transferred hydrogen had a very similar charge in both TS's (-0.47e *vs.* -0.49e for carbon and +0.44e for hydrogen), the hydroxide oxygen charge in TS IIIA-**1** was clearly larger (-1.14e) than that of the catalyst alkoxide oxygen (-0.92e) in TS IIIB-**1**. The delocalization of the oxygen negative charge by polarization in the much larger, and positively charged, catalyst moiety in the latter TS

can explain its stability. The same reasoning applies to the less stable TSIIIA-**2**, which shows an even more negative charge on the hydroxide oxygen (-1.20e), due to the lack of hydrogen bonding to the catalyst with respect to TSIIIA-**1**.

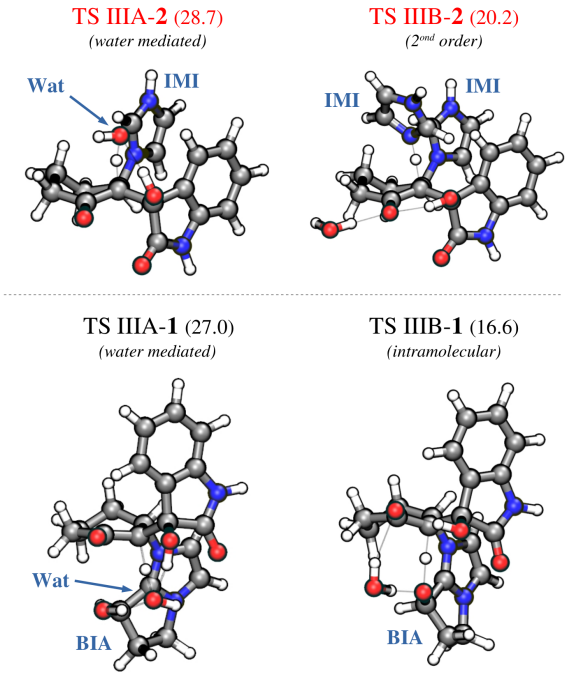

Figure 5. Optimized structures and energies (in kcal·mol^{-1}) of the four possible transition states of the proton transfer (step III in Scheme 2), according to the nature of the nucleophilic catalyst (imidazole or BIA) and to the identity of the proton-transfer agent (water or catalyst).

The stabilization of TSIII B-**1** is the most important reason for the higher catalytic efficiency of BIA with respect to imidazole. The kinetic improvement brought about by this catalyst-mediated proton transfer is also limited by the catalyst addition step, which is competitive with the proton transfer for α,β-unsaturated ketones. For common donors such as methyl acrylate this improvement should however be much higher. Note that this result also rationalizes the experimentally observed very low reaction rate measured with the O-methyl derivative **6**, for which the only possible mechanism available for the proton transfer is the water-mediated one, with an activation energy barrier of *ca.* 29 kcal·mol^{-1} from the separated reactants, that is 9 kcal mol^{-1} higher than that found for imidazole for this step (according to pathway B) and 5 kcal mol^{-1} higher than that of the catalyst addition step.

Although bifunctional Lewis base-Brønsted acid systems have been previously used as catalysts for the MBH or aza-MBH reactions of acrylates, particularly in their enantioselective variants,[6] we note that up to now no evidence has been found, either experimental[26,28] or theoretical,[14f,14g,29] for the direct participation of the hydrogen bond donor group of the catalyst in the proton transfer step. These results highlight the dramatic enhancement in catalytic efficiency caused by the addition to the catalyst structure of a functional group able to participate in a proton transfer process, even if the reaction occurs in water solution. Whereas this phenomenon is well known in enzymatic catalysis, it has not been previously noted in organocatalytic processes such as the MBH reaction.

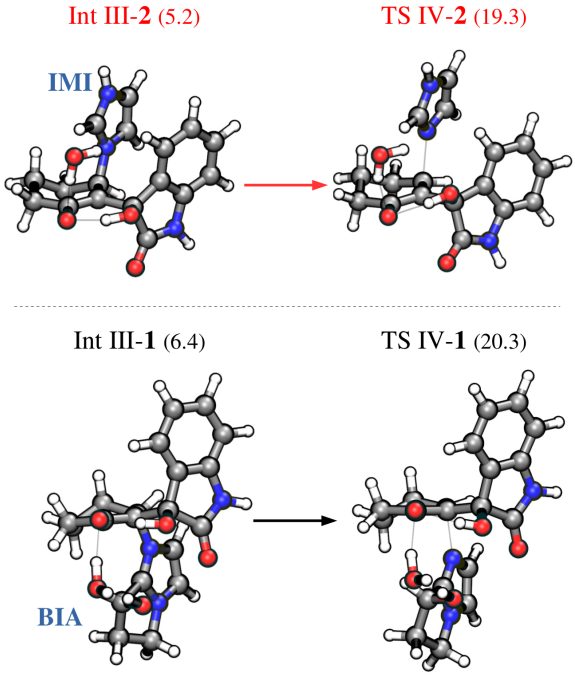

Figure 6. Free energies (in kcal·mol^{-1}) and optimized structures of the stationary points for the catalyst elimination (step IV in Scheme 2) of imidazole (IMI **2**; up) and BIA (**1**; down).

3.2.4. Step IV: Catalyst elimination and product release.

The last step of the MBH reaction (Scheme 2) involves the elimination of the catalyst moiety from the second zwitterionic intermediate (Int III-**1** or Int III-**2**), providing the final MBH adduct **5** and closing the catalytic cycle. This step is highly exoergic for both catalysts, with ΔG^0 = -7.2 kcal·mol^{-1} for imidazole and ΔG^0 = -8.4 kcal·mol^{-1} for BIA, and goes through TS IV-**2** and TS IV-**1**, respectively (Figure 6). In these TS's, the hydroxyl group of the oxindole moiety is involved in an intramolecular hydrogen bond with the carbonyl of the cyclohexanone fragment. For the BIA catalyst**,** this step has the second highest individual free energy barrier (ΔG = 13.9 kcal·mol^{-1}). For imidazole, the energy barrier is very similar ($\Delta G^{\ddagger}$ = 14.2 kcal·mol^{-1}). The formation of the adduct **5** from the reactants (**3** and **4**) is exergonic, defining a total ΔG^0 of -2 kcal·mol^{-1} for the overall MBH reaction.

3.3. ESI(+)-MS monitoring.

The *in situ* monitoring by ESI(+)-MS of the two reactions studied by theoretical calculations was also performed to try to intercept and characterize the main key intermediates. Figures 7a and 7b show, respectively, the spectra of the reaction mixture aliquots with imidazole **2** and of BIA **1** at times 0, 10 and 30 min. The beginning of the monitoring (t = 0 min) corresponds to a sample extracted from the homogeneous mixture obtained immediately after the addition of

reactants (**3**, **4**) and catalyst (**1** or **2**) to a magnetically stirred 10% mol aqueous solution of SDS. As predicted by the calculations, these spectra reveal indeed significant differences between the catalytic activities of **1** and **2**. At short reaction times, the abundances of the ions corresponding to the initial reaction intermediates are much lower for imidazole (Figure 7a) as compared to BIA (Figure 7b), in accordance with the higher catalytic activity of BIA. It can also be seen that the ion of *m/z* 148, corresponding to protonated isatin, cannot be detected, even at t = 0 min, in the BIA-catalyzed reaction (Figure 7b). The structures of the detected intermediates have been assigned by MS/MS experiments (see SI).

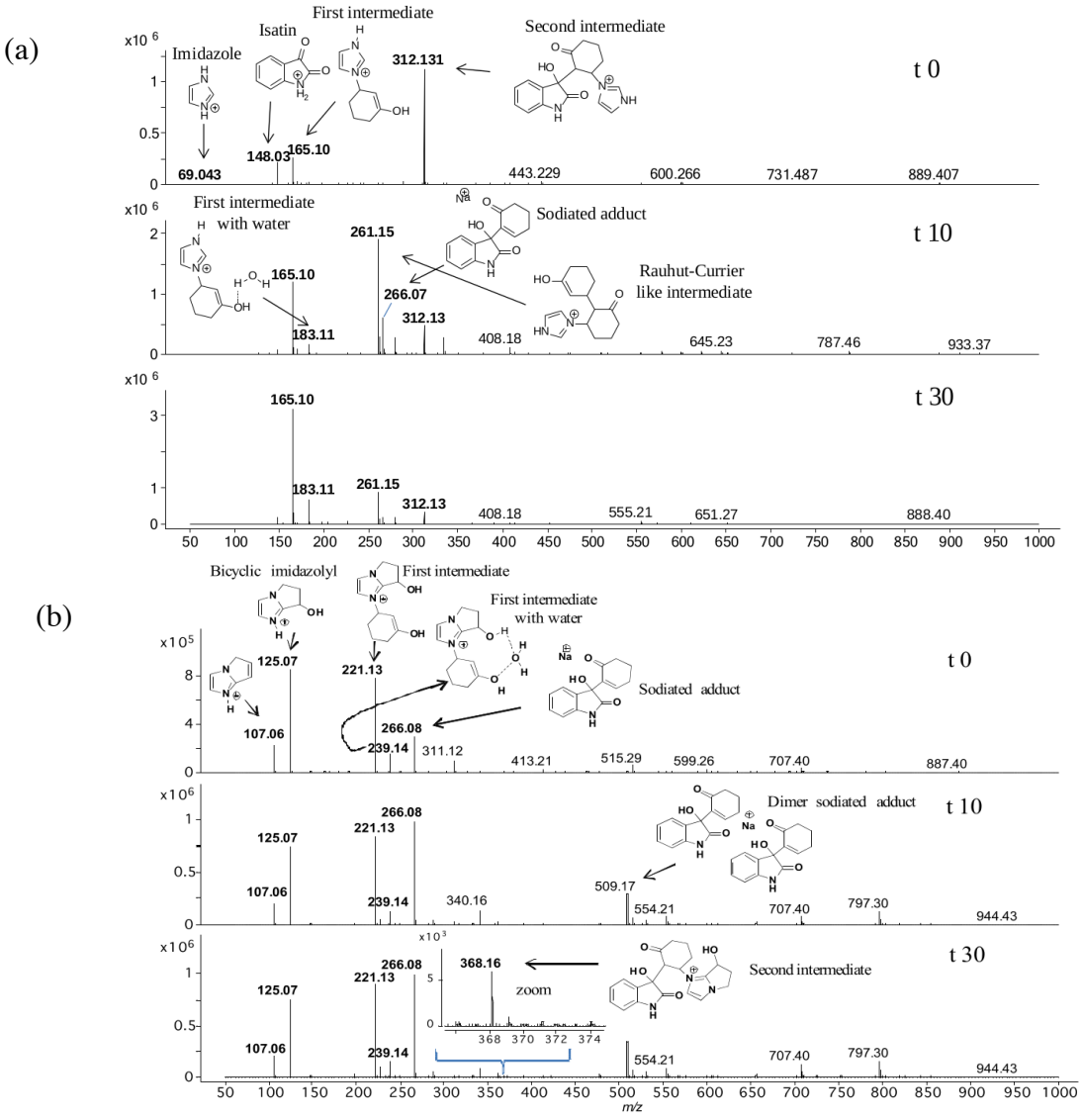

Figure 7. (a) ESI(+)-MS of the reaction solution of isatin **3**, 2-cyclohexenone **4** (2.0 equiv.) and imidazole **2** (0.10 equiv.) after mixing (t = 0 min, top), and after 10 min (middle) or 30 min (bottom) of reaction. (b) ESI(+)-MS of the reaction solution of isatin **3**, 2-cyclohexenone **4** (2.0 equiv.) and BIA **1** (0.10 equiv.) after mixing (t = 0 min, top), and after 10 min (middle) or 30 min (bottom) of reaction.

For the imidazole-catalyzed reaction, the ion of *m/z* = 165, corresponding to the protonated adduct of 2-cyclohexenone 4 with imidazole, is detected both at t = 0, t = 10 and t = 30 min). But the hydrated adduct ion of *m/z* = 183, which corresponds to intermediate II-2, is only detected at t = 10 and t = 30 min. The MS data reveal a different behavior for the BIA-catalyzed reaction, in which ion of *m/z* = 239 which corresponds to the hydrated adduct of the enone with the catalyst (intermediate Int II-1) is already detected at t = 0 (Figure 7b), an observation that supports its relative greater stability, predicted by the calculations. A most significant feature of the *in situ* ESI(+)-MS data is that, also at

short reaction times, the most abundant ion in the imidazole-catalyzed reaction is that of *m/z* 312, which corresponds to the protonated aldol adduct intermediate Int II-2 (Figure 7a). The corresponding ion of *m/z* 368 is on the contrary missing in the two first spectra of the BIA-catalyzed reaction collected at t = 0 and t = 10 min (Figure 7b). This perfectly matches the calculations, since if the proton transfer is the rate determining step in the imidazole-catalyzed reaction, an accumulation of this intermediate should occur at short reaction times. The abundance of the ion of *m/z* 312 diminishes with longer reaction times but it still can be detected at t = 30 min (Figure 7a, bottom).

The ion of *m/z* 266, corresponding to the sodiated final MBH adduct **5**, that is, [**5**+Na^+], initially detected as a very minor ion in the imidazole catalyzed reaction (Figure 7a, t = 10 min), is much more abundant, from t = 0, in the spectra of the BIA-catalyzed reaction (Figure 7b). In this case, at longer reaction times (t = 10 min and t = 30 min) the ion corresponding to [**5**+**5**+Na^+], of *m/z* = 509, is also detected, an evidence for the higher content of the final product in the reaction mixture.[30]

Finally, we also monitored by *in situ* ESI(+)-MS the evolution of an aqueous mixture of isatin **3** and 2-cyclohexanone **4**, in the presence of the O-methylated BIA derivative **6** (Figure 8). In this case, and due to the high abundance of the ion corresponding to protonated **6** (*m/z* = 139), the amount of catalyst had to be reduced 10 times with respect to the conditions used for the imidazole- and the BIA-catalyzed reactions. In agreement with our experimental findings of the very low reaction rate with this catalyst, the ion with *m/z* = 266 corresponding to the sodiated adduct was only detected in trace amounts after t = 30 min (not shown in Figure 8). The intermediate corresponding to the Michael addition of the catalyst (step I in Scheme 2) could be detected at t = 10 min, and at t = 30 min the ion of *m/z* = 382, corresponding to the protonated aldol intermediate, was present in the reaction mixture, albeit in very minor amounts. This demonstrates that for this catalyst the rate-determining step takes place *after* the aldol addition step (step II in Scheme 2), in complete agreement with the results of our calculations: the low efficiency of the methylated BIA derivative **6** results from a) the impossibility of promoting *intramolecularly* the proton-transfer step, and b) the steric hindrance that would be present in the transition state involving two molecules of catalyst (see path B in Scheme 4).

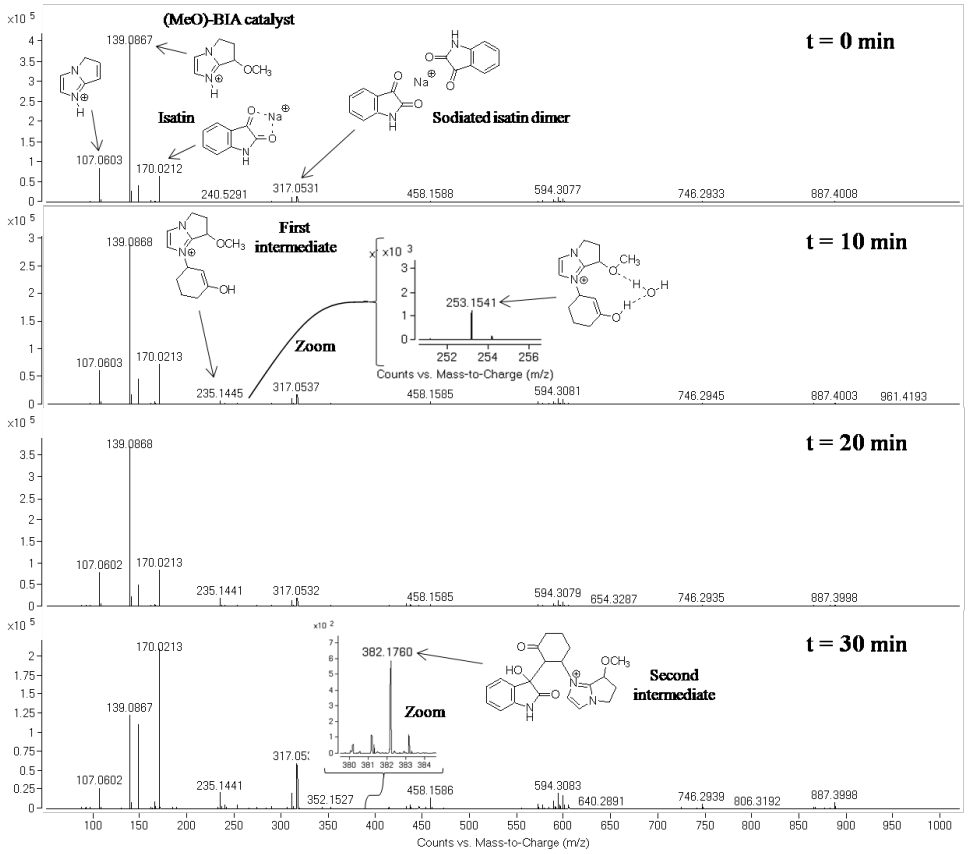

Figure 8. ESI(+)-MS of the reaction solution of isatin **3**, 2-cyclohexenone **4** (2.0 equiv.) and (OMe)-BIA **6** (0.01 equiv.) after mixing (t = 0 min, top), and after 10 min (middle) or 30 min (bottom) of reaction.

4. Final remarks and conclusions

The main goal of the present study was to explain why the presence of a hydroxyl group in the BIA catalyst **1** increases its catalytic efficiency in the MBH reaction of cyclic α,β-unsaturated ketones with respect to imidazole **2** in an aqueous solution. If we compare the two calculated free energy profiles shown in Figure 2, corresponding to the catalysis by **1** and **2** (second order pathway for the proton transfer step), several features are worth mentioning: First, the initial Michael addition of the catalyst to 2-cyclohexenone **4**, leading to an unstable zwitterionic enolate (Int I-**1**/**2**), has the largest individual energy barrier for both catalysts, and in fact it corresponds to the rate-determining step in the reaction catalyzed by the bicyclic imidazolyl alcohol **1**. Note that step I is not found to be rate-determining for the donor substrates most usually employed in mechanistic studies (experimental or theoretical) of the MBH reaction, which involve strong, β-unsubstituted Michael acceptors (*Cf.* methyl acrylate) and highly nucleophilic amine catalysts (*Cf.* DABCO). In the BIA-catalyzed reaction, both the transition state TS I-**1** and the resulting intermediate Int I-**1** are however more stable (by 1.7 and by 3.9 kcal·mol^{-1}, respectively) than the TS I-**2** and the intermediate Int I-**2**, corresponding to the catalysis by imidazole **2**. This stabilization order can be attributed to the action of the hydroxyl group of the catalyst as a hydrogen-bond donor to a solvent water molecule, stabilizing the negative charge on the oxygen enolate both in the TS and in the zwitterionic intermediate.[19] This extra-stabilization also affects the energies of the TS's of the aldol-type addition step (TS II-**1** and TS II'-**1**).

The most important difference between both catalysts is however found in the carbon-to-oxygen proton transfer step (Step III in Scheme 2). Our calculations show that although for imidazole the initial Michael addition of the catalyst still has the highest activation energy, no individual step is rate determining, and that the proton transfer step contributes to the overall rate of the process. In the BIA-catalyzed reaction proton transfer is much easier than the initial catalyst addition and not rate-limiting compared to imidazole. The presence of the hydroxyl group of the catalyst **1** triggers a stepwise acid-base mechanism for the proton transfer: the catalyst hydroxyl first donates a proton to the alkoxide group of the oxindole moiety in intermediate Int II-**1**, and then the resulting alkoxide Int II'-**1** abstracts the α–carbonylic proton. The water molecule only plays an ancillary role in this process, stabilizing the transition states and intermediates by hydrogen bonding. Our calculations show that an external water molecule could also play the role of the hydroxyl group, but in a much less efficient way as the corresponding process would be energetically much more demanding ($\Delta\Delta G^{\ddagger}$ = +10.4 kcal mol^{-1}). Although a direct comparison of the initial reaction rates cannot be made accurately, due to the lack of a single rate-determining step for the imidazole-catalyzed process, a reasonable estimate made on the basis of the differences in activation energy of the first step would give a $\Delta\Delta G^{\ddagger}$ of -1.7 kcal mol^{-1} between BIA and imidazole, that corresponds to a rate increase of 17.7, a predicted ratio reasonably close to that measured experimentally (k_{BIA}/k_{IMI} = 14.3).

The above theoretical results are also in good agreement with experimental ESI(+)-MS data. Moreover, they are also consistent with the recent study of the DABCO-catalyzed MBH reaction between methyl acrylate and 4-nitrobenzaldehyde in methanol by Plata and Singleton, that refutes the usual "proton-shuttle" pathway in favor of a two-step acid-base mechanism.[15] Another important conclusion of present study is the possibility of asymmetric induction by the chiral catalyst **1**, an issue that is currently being addressed in our laboratories.[31]

Finally, we have demonstrated that intramolecular hydrogen bonding by suitable functional groups in the catalyst can favorably compete with hydrogen bonding of the substrate with water in an aqueous reaction, leading to new reaction pathways that are lower in energy, just in the spirit of enzymatic catalysis.

ASSOCIATED CONTENT

Supporting Information

Additional experimental and computational details. This material is available free of charge via the Internet at http://pubs.acs.org.

AUTHOR INFORMATION

Corresponding Authors

*Albert Moyano (amoyano@ub.edu), Lluís Raich (lraich@ub.edu), Fernando Coelho (coelho@iqm.unicamp.br).

Author Contributions

The manuscript was written through contributions of all authors. Experimental work on the MBH reaction was performed by H. S. and J. C. G., under the supervision of A. M., F. C. and M. T. R. Theoretical calculations were performed by L. R., under the supervision of C. R. and A. M. MS/MS experiments were performed by R. G., under the supervision of M. N. E. A. M. and L. R. wrote and edited the manuscript which was corrected by C. R. and F. C. All authors have given approval to the final version of the manuscript.

Notes

The authors declare no competing interests.

Funding Sources

This work was supported by grants CTQ2014-55174 and CTQ2013-47401-C2-1-P (to C. R. and A. M., respectively) from MINECO, grants 2013/10449-5 ,2013/07600-3 and 2015/09205-0 (to H.S.) from FAPESP, grant 307840-2014-0 from CNPq (to F. C.), as well as grant 2014SGR-987 (to C. R.) from AGAUR.

ACKNOWLEDGMENT

We acknowledge the computer support of the Institut de Química Teòrica i Computacional (IQTCUB). L. R. thanks the University of Barcelona for an APIF fellowship.

ABBREVIATIONS

BIA, 7-hydroxy-6,7-dihydro-5*H*-pyrrolo[1,2-*a*]imidazole; DFT, density functional theory; ESI-MS, electrospray ionization mass spectrometry.

REFERENCES

(1) (a) Morita, K. Japan Patent 6803364, 1968. (b) Morita, K.; Suzuki, Z.; Hirose, H. *Bull. Chem. Soc. Jpn.* 1968, *41*, 2815-2815. (c) Baylis, A. B.; Hillman, M. E. D. German Patent 2155113,1972.

(2) (a) Ciganek, E. In *Organic Reactions*; Paquette, L. A., Ed.; John Wiley & Sons, Inc.: New York, 1997; Vol 51, pp. 201-350. (b) Basavaiah, D.; Rao, A. J.; Satyanarayana, T. T. *Chem. Rev.* 2003, *103*, 811-892.

(3) For recent reviews on the MBH or on the aza-MBH reaction see, among others: (a) Singh, V.; Batra, S. *Tetrahedron* 2008, *64*, 4511-4574. (b) Declerck, V.; Martínez, J.; Lamaty, F. *Chem. Rev.* 2009, *109*, 1-48. (b) Basavaiah, D.; Reddy, B. S.; Badsara, S. S. *Chem. Rev.* 2010, *110*, 5447-5674. (c) Shi, M.; Wang, F.-J.; Zhao, M.-X.; Wei, Y. *The Chemistry of the Morita–Baylis–Hillman Reaction*; RSC Publishing: Cambridge, U. K., 2011. (d) Wei, Y.; Shi, M. *Chem. Rev.* 2013, *113*, 6659-6690.

(4) Dunn, P. J.; Hughes, M. L.; Searle, P. M.; Wood, A. S. *Org. Proc. Res. Dev.* 2003, *7*, 244-253.

(5) (a) Reddy, Y. S.; Kadigachalam, P.; Basak, R. K.; John Pal, A. P.; Vankar, Y. D. *Tetrahedron Lett.* 2012, *53*, 132-136. (b) Paioti, P. H. S.; Coelho, F. *Tetrahedron Lett.* 2011, *52*, 6180-6184. (c) Kumar, V.; Das, P.; Ghosal. P.; Shaw, A. K. *Tetrahedron* 2011, *67*, 4539-4546. (d) Reddy, R. L.; Saravanan, P.; Corey. E. J. *J. Am. Chem. Soc.* 2004, *126*, 6230-6231; (e) Iwabuchi, Y.; Furukawa, M.; Esumi, T.; Hatakeyama, S. *Chem. Commun.* 2001, 2030-2031. (f) Luna-Freire, K. R.; Tormena, C. F.; Coelho, F. *Synlett* 2011, 2059-2063. (g) Gowrisankar, S.; Lee, H. S.; Kim, S. H.; Lee, Y. K.; Kim, J. N. *Tetrahedron* 2009, *43*, 8769-8780. (h) Teodoro, B. V. M.; Correia, J. T. M.; Coelho, F. *J. Org. Chem.* 2015, *80*, 2529-2538.

(6) (a) Iwabuchi, Y.; Nakatani, M.; Yokoyama, N.; Hatakeyama, S. *J. Am. Chem. Soc.* 1999, *121*, 10219-10220. (b) Mansilla, J.; Saá, J. M. *Molecules* 2010, *15*, 709-734. (c) Hatakeyama, S. In *Science of Synthesis, Asymmetric Organocatalysis 1: Lewis Base and Acid Catalysis*; List, B. Ed.; Thieme, Suttgart: 2012, pp 673-721. (d) Nakamoto, Y.; Urabe, F.; Takahashi, K.; Ishihara, J.; Hatakeyama, S. *Chem. Eur. J.* 2013, *19*, 12653-12656. (e) Wei, Y.; Shi, M. In *Comprehensive Enantioselective Organocatalysis. Volume 3: Reactions and Applications*; Dalko, P. I., Ed.; Wiley-VCH, Weinheim: 2013, pp 899-939.

(7) (a) Luo, S.; Mi, X.; Xu, H.; Wang, P. G.; Cheng, J.-P. *J. Org. Chem.* 2004, *69*, 8413-8422. (b) Basavaiah, D.; Roy, S.; Das, U. *Tetrahedron* 2010, *66*, 5612-5622.

(8) (a) Gatri, R.; El Gaïed, M. M. *Tetrahedron Lett*. 2002, *43*, 7835-7836. (b) Luo, S.; B. Zhang, B.; He, J.; Janczuk, A.; Wang, P. G.; Cheng, J.-P. *Tetrahedron Lett*. 2002, *43*, 7369-7371. (c) Luo, S.; Wang, P. G.; Cheng, J.-P. *J. Org. Chem*. 2004, 69, 555-558. (d) Porzelle, A.; Williams, C. M.; Schwartz, B. D.; Gentle, I. R. *Synlett* 2005, 2923-2926. (e) Schwartz, B. D.; Porzelle, A.; Jack, K. S.; Faber, J. M.; Gentle, I. R.; Williams, C. M. *Adv. Synth. Catal.* 2009, *351*, 1148-1154. See also: (f) Pawar, B.; Padalkar, V.; Phatanguare, K.; Nirmalkar, S.; Chaskar, A. *Catal. Sci. Technol*. 2011, *1*, 1641-1644.

(9) (a) Hill, J. S.; Isaacs, N. S. *J. Phys. Org. Chem.*1990, *3*, 285-288. (b) Santos, L. S.; Pavam, C. H.; Almeida, W. P.; Coelho, F.; Eberlin, M. N. *Angew. Chem. Int. Ed. Engl.* 2004, *43*, 4330-4333. (c) Cantillo, D.; Kappe, C. O. *J. Org. Chem.* 2010, *75*, 8615-8626. (d) Rodrigues, T. S.; Siva, V. H. C.; Lalli, P. M.; de Oliveira, H. C. B.; da Silva, W. A.; Coelho, F.; Eberlin, M. N.; Neto, B. A. D. *J. Org. Chem.* 2014, *79*, 5239-5248.

(10) Hoffmann, H. M. R.; Rabe, J. *Angew. Chem. Int. Ed. Engl.* 1983, *22*, 795-796.

(11) Aggarwal, V. K.; Fulford, S. Y.; Lloyd-Jones, G. C. *Angew. Chem. Int. Ed. Engl.* 2005, *44*, 1706-1708.

(12) (a) Price, K. E.; Broadwater, S. J.; Walker, B. J.; McQuade, D. T. *J. Org. Chem.* 2005, *70*, 3980-3987. (b) Price, K. E.; Broadwater, S. J.; Jung, H. M.; McQuade, D. T. *Org. Lett.* 2005, *7*, 147-150.

(13) (a) Amarante, G. W.; Benassi, M.; Sabino, A. A.; Esteves, P. M.; Coelho, F.; Eberlin, M. N. *Tetrahedron Lett.* 2006, *47*, 8427-8431. (b) Amarante, G. W.; Milagre, H. M. S.; Vaz, B. G.; Ferreira, B. R. V.; Eberlin, M. N.; Coelho, F. *J. Org. Chem.* 2009, *74*, 3031-3037. (c) Amarante, G. W.; Benassi, M.; Sabino, A. A.; Esteves, P. M.; Eberlin, M. N.; Coelho, F. *Tetrahedron* 2010, *66*, 4370-4376. For a recent kinetic study of the aza-MBH reaction, including some computed structures, see: (d) Lindner, C.; Liu, Y.; Karaghiosoff, K.; Maryasin, B.; Zipse, H. *Chem. Eur. J.* 2013, *19*, 6429-6434.

(14) See: (a) Xu, J., *J. Mol. Struct. THEOCHEM* 2006, *767*, 61-66. (b) Robiette, R.; Aggarwal, V. K.; Harvey, J. N. *J. Am. Chem. Soc.* 2007, *129*, 15513-15525. (c) Fan, J.-F.; Yang, C.-H.; He, L.-J. *Int. J. Quantum Chem.* 2009, *109*, 1311-1321. (d) Li, J.; Jiang, W.-Y. *J. Theor. Comput. Chem.* 2010, *9*, 65-75. (e) Roy, D.; Patel, C.; Sunoj, R. B. *J. Org. Chem.* 2009, *74*, 6936-6943. (f) Dong, L.; Qin, S.; Su, Z.; Yang, H.; Hu, C. *Org. Biomol. Chem.* 2010, *8*, 3985-3991. For a recent theoretical study on the aza-MBH reaction, see: (g) Lee, R.; Zhong, F.; Zheng, B.; Meng, Y.; Lu, Y.; Huang, K.-W. *Org. Biomol. Chem.* 2013, *11*, 4818-4824.

(15) Plata, R. E.; Singleton, D. A. *J. Am. Chem. Soc.* 2015, *137*, 3811-3826.

(16) Winter, A. *Nature Chem*. 2015, *7*, 473-475.

(17) (a) Weintraub, P. M.; Tiernan, P. L.; Huffman, J. C. *J. Heterocyclic Chem*. 1987, *24*, 561-563. (b) Zhang, Z. F.; Xie, F.; Jia, J.; Zhang, W. B. *J. Am. Chem. Soc*. 2010, *132*, 15939-15941.

(18) Gomes, J. C.; Rodrigues Jr., M. T.; Moyano, A.; Coelho, F. *Eur. J. Org. Chem.* 2012, 6861-6866.

(19) Gomes, J. C.; Sirvent, J.; Moyano, A.; Rodrigues Jr., M. T.; Coelho, F. *Org. Lett.* 2013, *15*, 5838-5841.

(20) Gaussian 09, Revision D.01, Frisch, M. J.; Trucks, G. W.; Schlegel, H. B.; Scuseria, G. E.; Robb, M. A.; Cheeseman, J. R.; Scalmani, G.; Barone, V.; Mennucci, B.; Petersson, G. A.; Nakatsuji, H.; Caricato, M.; Li, X.; Hratchian, H. P.; Izmaylov, A. F.; Bloino, J.; Zheng, G.; Sonnenberg, J. L.; Hada, M.; Ehara, M.; Toyota, K.; Fukuda, R.; Hasegawa, J.; Ishida, M.; Nakajima, T.; Honda, Y.; Kitao, O.; Nakai, H.; Vreven, T.; Montgomery, Jr., J. A.; Peralta, J. E.; Ogliaro, F.; Bearpark, M.; Heyd, J. J.; Brothers, E.; Kudin, K. N.; Staroverov, V. N.; Kobayashi, R.; Normand, J.; Raghavachari, K.; Rendell, A.; Burant, J. C.; Iyengar, S. S.; Tomasi, J.; Cossi, M.; Rega, N.; Millam, J. M.; Klene, M.; Knox, J. E.; Cross, J.; Bakken, B.; Adamo, C.; Jaramillo, J.; Gomperts, R.; Stratmann, R. E. V.; Yazyev, O.; Austin, A. J.; Cammi, R.; Pomelli, C.; Ochterski, J. W.; Martin, R. L.; Morokuma, K.; Zakrzewski, V. G.; Voth, G. A.; Salvador, P.; Dannenberg, J. J.; Dapprich, S.; Daniels, A. D.; Farkas, Ö.; Foresman, J. B.; Ortiz, J. V.; Cioslowski, J.; Fox, D. J. Gaussian, Inc., Wallingford CT, 2009.

(21) Hohenberg P.; Kohn, W. *Phys. Rev.* 1964, *136*, B864-B871.

(22) Zhao Y.; Truhlar, D. G. *Theor. Chem. Acc.,* 2008, *120*, 215-241.

(23) Kohn W.; Sham, L. J. *Phys. Rev.* 1965, *140*, A1133-A1138.

(24) Krenske, E. H.; Petter, R. C.; Zhu, Z.; Houk, K. N. *J. Org. Chem*. 2011, *76*, 5074-5081.

(25) Marenich, A. V.; Cramer, C. J.; Truhlar, D. G. *J. Phys. Chem. B* 2009, *113*, 6378-6396.

(26) Aggarwal, V. K.; Emme, I.; Fulford, S. Y. *J. Org. Chem.* 2003, *68*, 692-700.

(27) Anslyn, E. V.; Dougherty, D. A. *Modern Physical Organic Chemistry*; University Science Books, 2006. Section 5.3.2, pp. 273-275.

(28) (a) Ameer, F.; Drewes, S. E.; Freese, S. D.; Kaye, P. T. *Synth. Commun.* 1988, *18*, 495-500. (b) Drewes, S. E.; Freese, S.

D.; Emslie, N. D.; Roos, G. H. P. *Synth. Commun.* 1988, *18*, 1565-1572.
(29) Martelli, G.; Orena, M.; Rinaldi, S. *Eur. J. Org. Chem.* 2012, 4140-4152.
(30) Other species that can be identified in the spectra, but that do not play a direct role in the mechanism, are a protonated Rauhut-Currier intermediate (*m/z* = 261, Figure 7(a) middle and bottom) and the ion of *m/z* = 368 that can be identified, albeit with very low intensity, in the last spectrum of the BIA-catalyzed reaction (Figure 7(b), bottom). Although its mass coincides with that of the protonated aldol adduct Int II-**1**, this species probably arises from the Michael addition of the catalyst **1** to the MBH adduct **5**, *i.e.* to the protonated form of the intermediate Int III-**1**. The structural assignments of the main key intermediates are supported both by HRMS data and tandem MS spectra (see SI). For reviews on the Rauhut-Currier reaction, see: (a) Aroyan, C. E.; Demenci, A.; Miller, S. J. *Tetrahedron* 2009, *65*, 4069-4084. (b) Xie, P.; Huang, Y. *Eur. J. Org. Chem*. 2013, 6213-6226.
(31) This issue is currently being investigated in our laboratories, and the results will be published in due course. Preliminary experiments carried out with enantiomerically enriched (> 99% ee) BIA catalyst **1** show that under the standard reaction conditions the MBH adduct **5** is obtained with at least 46% ee. For the enzymatic resolution of **1**, see: De Miranda, A.; Gomes, J. C.; Rodrigues Jr., M. T.; Costa, I. C. R.; Almeida, W. P.; Lopes, R.; Miranda, L. S. M.; Coelho, F.; de Souza, R. O. M. A. *J. Mol. Catal. B: Enzym.* 2013, *91*, 77-80.

SYNOPSIS TOC